Interface electronic structure of alkanethiolate-passivated Au nanoparticles studied by photoelectron spectroscopy

Tanaka, Akinori
Imamura, Masaki
Yasuda, Hidehiro

(Citation)
Physical Review B,74(11):113402-113402

(Issue Date)
2006-09-12

(Resource Type)
journal article

(Version)
Version of Record

(URL)
https://hdl.handle.net/20.500.14094/90000099

Interface electronic structure of alkanethiolate-passivated Au nanoparticles studied by photoelectron spectroscopy

Akinori Tanaka,[1,2,*] Masaki Imamura,[2] and Hidehiro Yasuda[1,2]
[1]*Department of Mechanical Engineering, Faculty of Engineering, Kobe University, Nada-ku, Kobe 657-8501, Japan*
[2]*Department of Mechanical and Systems Engineering, Graduate School of Science and Technology, Kobe University, Nada-ku, Kobe 657-8501, Japan*

(Received 17 April 2006; revised manuscript received 16 June 2006; published 12 September 2006)

We have carried out the photoemission study of various alkanethiolate- (AT-) passivated Au nanoparticles. From the detailed line-shape analyses of Au 4*f* core-level photoemission spectra, it is found that the interface chemical states are independent on the surface passivants of AT molecules among the AT-passivated Au nanoparticles with the same size. Moreover, the interface electronic structures of AT-passivated Au nanoparticles have been characterized. It is found that the surface-potential shifts due to the interface dipoles accompanying the adsorption of AT molecules are about 0.36 eV and are independent on the surface passivants of AT molecules. The detailed interface electronic state of AT-passivated Au nanoparticle is discussed.

DOI: 10.1103/PhysRevB.74.113402 PACS number(s): 73.22.−f, 73.90.+f

Metallic nanoparticles are attracting much interest from the viewpoints of both device and fundamental physics, because they show distinctive physical and chemical properties found in neither bulk nor molecular/atomic systems, such as high catalytic activity[1] and Coulomb blockades.[2] Recently, the inorganic nanoparticles surface-passivated by organic molecules have been chemically synthesized in the solution,[3,4] and these are monodisperse and stable even at room temperature. Therefore, these surface-passivated nanoparticles are suitable for the study of their fundamental size-dependent properties and functions. Furthermore, it has been reported that these surface-passivated nanoparticles exhibit closed-packed nanoparticle self-assemblies on the single-crystalline substrates.[5,6] Therefore, it is considered that they could be important constituents of the future nanostructured devices, such as single-electron devices, catalysts, and ultrahigh-density memory. Upon these applications, the interface properties play a key role to control energetic barriers to charge injection. In this work, we have carried out a photoemission study of the various alkanethiolate- (AT-) passivated Au nanoparticles. The present work elucidates the fundamental interface properties associated with AT termination in AT-passivated Au nanoparticles from the results of synchrotron-radiation core-level and ultraviolet photoemission studies.

The AT-passivated Au nanoparticles were synthesized by the method developed by Lin *et al.*[7] Firstly, didodecyldimethylammonium bromide was added to toluene and deionized water in order to form an inverse micelle system. After that, gold chloride was dissolved in this micelle solution by sonication. After a $NaBH_4$ aqueous solution was added to the above solution with stirring, Au nanoparticles were obtained. After the alkanethiols [octanethiol ($C_8H_{17}SH$, denoted by OT), dodecanethiol ($C_{12}H_{25}SH$, denoted by DT), and hexadecanethiol ($C_{16}H_{33}SH$, denoted by HDT)] was added as a surface passivant, Au nanoparticles were precipitated with ethanol and the bottom precipitates were dried under the vacuum. Then the dried precipitates were redispersed in toluene. The product was diluted in boiling toluene and left 1 day. The toluene/nanoparticle-rich phase was corrected and evaporated in a rotary evaporator, and then was washed with ethanol to remove the excess alkanethiol and reaction byproducts. After that, the product was redispersed in toluene, and finally highly monodispersed AT-passivated Au nanoparticles were obtained. The size distributions in diameter and shapes of thus synthesized AT-passivated Au nanoparticles were characterized by *ex situ* observations with a JEM-2000EXII (JEOL Co.) transmission electron microscope (TEM). The samples for TEM observations were prepared by evaporating the toluene dispersions of AT-passivated Au nanoparticles on the amorphous carbon-coated copper TEM grids. The obtained mean diameters from TEM observations of OT-, DT-, and HDT-passivated Au nanoparticles used in this work are 4.2, 4.1 nm, and 3.8 nm, respectively. The standard deviations of OT-, DT-, and HDT-passivated Au nanoparticles are 0.28, 0.38, and 0.4 nm, respectively. As s further characterization, the optical absorption measurements were performed using the V-570 (JASCO Co.) spectrometer. Photoemission measurements using synchrotron radiation were carried out at BL-5U of UVSOR II Facility, Institute for Molecular Science, Okazaki, Japan. Synchrotron radiation photoemission measurements were performed using A-1 (MBS-Toyama Co.) photoelectron spectrometer with incident photon energy of 190 eV at room temperature. Ultraviolet photoemission spectroscopy (UPS) measurements were performed at Kobe University using ARUPS 10 (VG Microtech Co.) photoelectron spectrometer with the He I resonance line ($h\nu$=21.2 eV) as the excitation source. For UPS measurements, the sample was biased with −5 V to reduce the effects of stray fields and to improve the determination of the energy of low kinetic-energy edge. The total-energy resolutions for synchrotron radiation photoemission and UPS measurements were about 150 and 70 meV, respectively. For all photoemission measurements, the synthesized AT-passivated Au nanoparticles were supported on the highly oriented pyrolytic graphite (HOPG) substrates by evaporating the solvent (toluene) from the dispersion of AT-passivated Au nanoparticles on the single-crystalline HOPG cleaved surface in a nitrogen-filled glove bag directly connected to the ultrahigh-vacuum photoelectron spectrometer. Then the samples were transferred into the photoemission analysis chamber without exposure to air. The thus-prepared

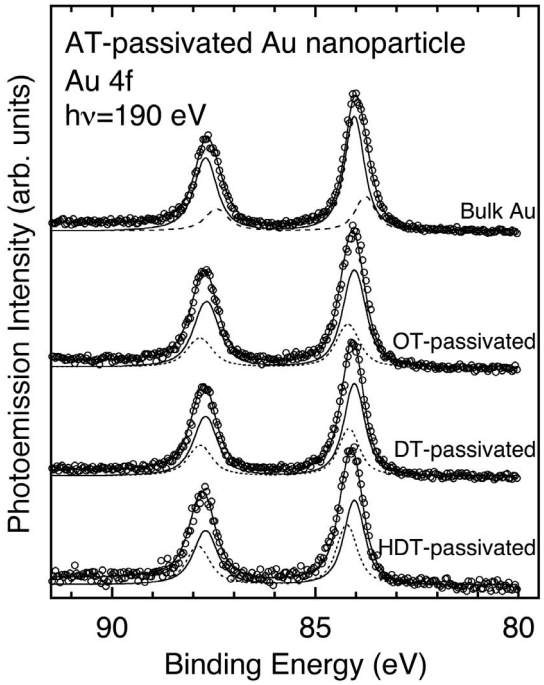

FIG. 1. Au 4*f* core-level photoemission spectra of AT-passivated Au nanoparticles measured with photon energy of $h\nu$=190 eV. The surface passivant is indicated on each spectrum. The mean diameters of OT-, DT-, and HDT-passivated Au nanoparticles are 4.2, 4.1 nm, and 3.8 nm, respectively. The top spectrum shows the Au 4*f* core-level spectrum observed for bulk Au polycrystalline evaporated film for a comparison. The observed spectrum of bulk Au crystallite is decomposed into bulk (solid line) and surface (dashed line) components, and those of all AT-passivated Au nanoparticles are decomposed into bulk components (solid lines) and interface components bonded to surface AT molecules (dotted lines).

samples show no Auger and x-ray photoemission signals from the contaminants. All the photoemission spectra showed no change in the course of the measurements.

Figure 1 shows Au 4*f* core-level photoemission spectra using synchrotron radiation of AT-passivated Au nanoparticles with the various AT surface passivants with mean diameters of about 4 nm measured with photon energy of $h\nu$ =190 eV. In Fig. 1, Au 4*f* core-level photoemission spectra of bulk Au polycrystalline evaporated film is also shown for a comparison (top spectrum in Fig. 1). Figure 1 also shows the results of line-shape analyses for Au 4*f* core-level spectra of AT-passivated Au nanoparticles and bulk Au polycrystallite. In Fig. 1, each decomposed peak was described by a convolution of Doniach-Sunjic line shape with a Gaussian due to the instrumental and phonon broadening. The detailed procedure of these line-shape analyses for Au 4*f* core-level photoemission spectra have been described elsewhere.[8,9] As previously well established,[8–11] Au 4*f* core-level photoemission spectrum of bulk Au crystallite is composed of two components, which originate from the Au atoms in the bulk (bulk component) and topmost surface Au layer (surface component). The surface core-level shift of −0.28 eV obtained from the present line-shape analysis for a photoemission spectrum of bulk Au crystallite is found to be consistent with the literature values.[8–11] In the Au 4*f* core-level photoemission spectrum of bulk Au crystallite, the components with higher binding energy (solid line in the top spectra of Fig. 1) and lower binding energy (dashed line in the top spectra of Fig. 1) are bulk and surface components, respectively. On the other hand, it is found that all the Au 4*f* core-level photoemission spectra of the present AT-passivated Au nanoparticles are also represented by two components. We have already reported in previous papers that Au 4*f* core-level photoemission spectra of DT-passivated Au nanoparticles are represented by two components.[8,9] In our previous works,[8,9] it was found that the relative intensity of higher binding-energy component to lower binding-energy component increases with decreasing the nanoparticle diameter. The nanoparticle systems have a higher number ratio of surface atoms to atoms in bulk with decreasing the nanoparticle diameter. Moreover, the binding energy and spectral feature of the lower binding-energy component are similar to those of bulk component in the Au 4*f* core-level photoemission spectrum observed for bulk Au crystallite. From these discussions, it has been concluded in the previous work that the components with lower binding energy and higher binding energy in the Au 4*f* core-level photoemission spectra of DT-passivated Au nanoparticles originate from the inner Au atoms of Au nanoparticles (bulk component) and the surface Au atoms of Au nanoparticles bonded to surface passivants of DT molecules (interface component), respectively. Therefore, the components with lower binding energy (solid lines) and higher binding energy (dotted lines) in the present Au 4*f* core-level photoemission spectra of OT- and HDT-passivated Au nanoparticles is also concluded to originate from the bulk component and interface component, respectively. The reason the relative intensity of the interface component to bulk component increases with increasing the molecular length of AT surface passivants (from OT to HDT) is that the contribution from the inner Au atoms of Au nanoparticle to photoemission spectra (bulk component) decreases with the increasing molecular length of AT surface passivants due to the extremely short mean free path of emitted photoelectron. In the previous work,[9] we have already discussed the chemical states and the size dependence of the DT-passivated Au nanoparticle from the chemical shift of interface component. Here, an important point to note is that the chemical shifts of these interface components are the same among the present AT-passivated Au nanoparticles with the same nanoparticle sizes. This means that the chemical features at the interface between Au nanoparticle and surface passivants of AT molecules, such as the charge transfer from Au nanoparticle to AT molecules, show no surface-passivant dependence among the present AT-passivated Au nanoparticles with the same sizes. This indicates that the interface dipoles induced by charge transfer from core Au to S (Au^{+}-S^{-} dipoles), as described below, are almost same among the present AT-passivated Au nanoparticles.

In order to investigate the interface properties of the present AT-passivated Au nanoparticles in more details, we have carried out the UPS measurements in the low kinetic-energy region. Figure 2 shows the UPS spectra in the low kinetic-energy region of AT-passivated Au nanoparticles with the He I resonance line ($h\nu$=21.2 eV), compared with that of bulk Au polycrystalline evaporated film. In Fig. 2, the low

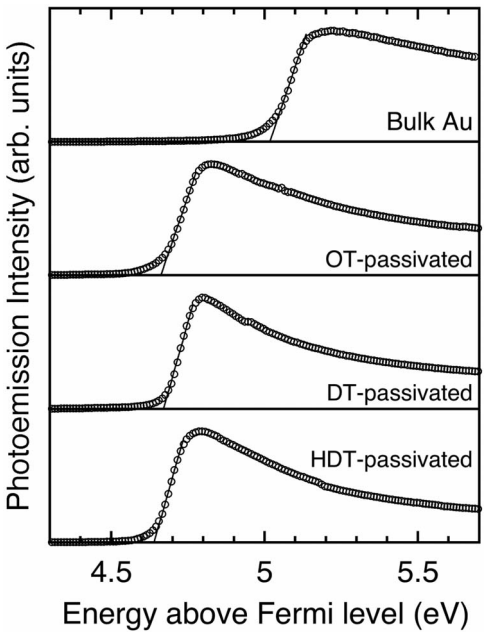

FIG. 2. Ultraviolet photoemission spectra in the vicinity of the vacuum level of AT-passivated Au nanoparticles supported on the HOPG substrates with the He I resonance line ($h\nu$=21.2 eV). The surface passivant is indicated on each spectrum. The mean diameters of OT-, DT-, and HDT-passivated Au nanoparticles are 4.2, 4.1 nm, and 3.8 nm, respectively. The top spectrum shows the spectrum observed for bulk Au polycrystalline evaporated film for a comparison.

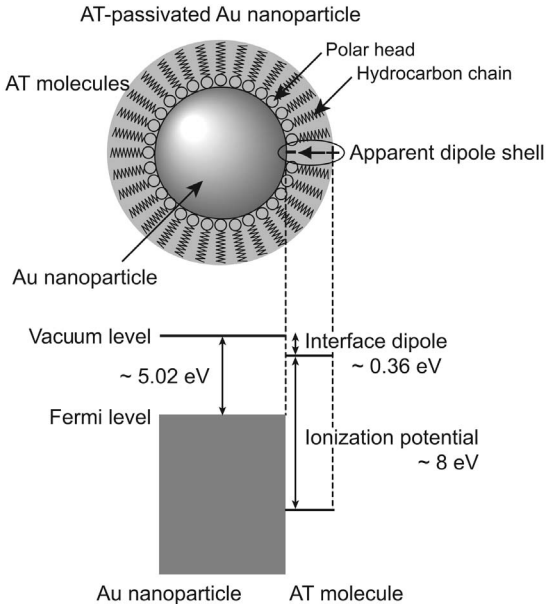

FIG. 3. Energy diagram of interface electronic structure in the AT-passivated Au nanoparticle with mean diameter of about 4 nm determined from the UPS measurements.

kinetic-energy edge of each UPS spectrum corresponds to the cutoff due to the vacuum level of each sample. Therefore, we have estimated the effective work function of each sample as an intersection point of horizontal axis and extrapolated line from the photoemission onset as shown in Fig. 2. From the top spectrum in Fig. 2, the obtained work function of bulk Au polycrystallite of 5.02 eV is found to be consistent with the literature values. On the other hand, the obtained effective work functions of the present OT-, DT-, and HDT-passivated Au nanoparticles are found to be 4.66, 4.67, and 4.64 eV, respectively. It is found that the obtained effective work functions of the present AT-passivated Au nanoparticles with mean diameters of about 4 nm are smaller than that of bulk Au crystallite and show no AT surface-passivant dependence. It has been confirmed to date that the electronic structures of the Au nanoparticles with diameter above ~2 nm remain metallic features. Of course, the optical extinction spectra of all the present AT-passivated Au nanoparticles exhibit the distinctive Mie plasmon resonance around 2.45 eV photon energy, indicative of a collective motion of valence electrons typical for a metallic material.[12] Moreover, it has been reported that the ionization potentials (that is, work functions) in the relevant nanoparticle-size regime of the present work are almost same as that of bulk Au crystallite.[13] Therefore, the energy diagram of interface electronic structures in the present AT- (OT-, DT-, and HDT-) passivated Au nanoparticles with mean diameters of about 4 nm can be described as shown in Fig. 3. In Fig. 3, the ionization potential of about 8 eV of AT surface-passivant molecules is derived from the results of the previous gas-phase UPS studies for AT molecules.[14] From this energy diagram, it is found that the change in surface potential due to the interface dipoles accompanying adsorption of AT molecules is about −0.36 eV and almost same among the present OT-, DT-, and HDT-passivated Au nanoparticles. Previously, Alloway *et al.*[14] have reported a surface potential shifts of self-assembled monolayers (SAMs) of various AT molecules on the Au substrates from the UPS studies. In their work, it was reported that the effective work functions of Au surfaces modified with SAMs of propanethiol (C_3H_7SH), OT, decanethiol ($C_{10}H_{21}SH$), HDT, and octadecanethiol ($C_{18}H_{37}SH$) are significantly small compared with that of bulk Au crystallite, and linearly decrease with AT molecular length. Consequent surface-potential shifts due to the adsorption of AT SAMs change from ~−1 eV to ~−1.3 eV with carbon number in AT molecular, 19 mV/CH_2 unit.

Compared with the previous results of AT SAMs on the Au surface, the present surface-potential shifts of AT-passivated Au nanoparticles with mean diameters of about 4 nm are significantly smaller than those of AT SAMs on the Au substrates, and show no dependence on the AT surface passivants' molecule length (the carbon number in surface passivants of AT molecules). The AT SAMs on the metallic substrate are considered to form the dipole sheet that is composed of dipoles of the hydrocarbon-chain region and head-group region of AT molecules. However, it has been already confirmed that the effective R^+-S^- dipole of the hydrocarbon-chain region (where R=C_nH_{2n+1}) is significantly larger than the Au^+-S^- dipole of the head-group region.[14,15] Therefore, the dipole of the hydrocarbon-chain region dominates, and AT SAMs on the flat metallic substrate form the *apparent* dipole sheet with a sheet of negative charges residing close to the SAM/metal interface and a sheet of positive charges closer to the vacuum/SAM interface. This induces the negative shifts in surface potential. By analogy with a parallel-

plate capacitor, the change in metal surface-potential due to this *apparent* dipole sheet in the case of SAMs on flat metallic substrate is given by $\Delta U_{\mathrm{SAM}}=l_{\mathrm{SAM}}\sigma/\varepsilon$, where l_{SAM} is the thickness of the *apparent* dipole sheet (that is, thickness of AT SAMs), σ is the areal density of charge, and ε is the static dielectric constant of AT SAMs. On the other hand, the present AT molecular layer terminated with Au nanoparticle can be considered as a spherical capacitor. In this case, the change in surface potential ΔU_{NP} of metal nanoparticle due to the *apparent* spherical dipole layer is described by

$$\Delta U_{NP}=\frac{q}{4\pi\varepsilon}\frac{l_{mol}}{r(r+l_{mol})}, \tag{1}$$

where q is the charge residing the spherical dipole shell, l_{mol} is the thickness of the *apparent* dipole layer (that is, AT molecules terminated with Au nanoparticle), and r is the radius of core Au nanoparticle. Alloway *et al.*[14] have reported the experimental surface-potential shifts (shifts in effective vacuum level from that of bulk Au crystallite) of −1.17 and −1.35 eV for OT and HDT SAMs on the Au substrates, respectively. That is, the surface-potential change of 0.18 eV from OT to HDT terminations has been observed for AT SAMs on the Au substrates. On the other hand, the present surface potentials of OT- and HDT-passivated Au nanoparticles are almost same, as described above. Assuming that Au-S interactions and adsorption densities of AT surface passivants in the AT-passivated Au nanoparticles are similar to those of AT SAMs on the Au substrates and consequent areal density of charge in the *apparent* dipole shell is same as that of *apparent* dipole sheet of AT SAMs on the Au substrate, that is $q=4\pi r^2\sigma$, the surface-potential shifts of AT-passivated Au nanoparticles are represented as $\Delta U_{\mathrm{NP}}=\Delta U_{\mathrm{SAM}}r/r+l_{mol}$. In this equation, we have experimentally measured the thickness of AT layers l_{mol} as half of the mean interparticle distance by TEM observations. This mean interparticle distance is determined from the interparticle distance distribution within the closed-packed self-assembled regions, which is considered to be an intrinsic nanoparticle distance.

Under these assumptions, we estimate the surface-potential shifts of 0.88 and 0.88 eV for the present OT- and HDT-passivated Au nanoparticles. These values are significantly smaller than corresponding AT SAMs on the Au substrates and show no surface-passivant dependence. Therefore, it is concluded that the experimental significantly smaller surface-potential shifts of AT-passivated Au nanoparticles than that of planer AT SAMs on the Au substrates and no dependence on the AT surface passivants can be qualitatively explained by the difference of the shape of interface dipole layer. However, the estimated surface-potential shifts of AT-passivated Au nanoparticles are not quantitatively consistent with the present experimental ones. This means that the areal density of charge in the dipole layer, that is, the bonding nature between surface passivants of AT molecules and Au nanoparticle surface, of AT-passivated Au nanoparticles is different from those of AT SAMs on the Au substrates.

In summary, we performed the synchrotron-radiation core-level photoemission and UPS studies of various AT-passivated Au nanoparticles. From the detailed line-shape analyses of Au $4f$ core-level photoemission spectra, it is found that the interface chemical states are independent of the AT surface passivants among the present AT-passivated Au nanoparticles with the same size. Moreover, the detailed interface electronic structures and surface potentials of AT-passivated Au nanoparticles have been characterized from the UPS spectra in the vicinity of vacuum level. It is found that the surface-potential shifts due to the interface dipoles accompanying adsorption of AT molecules are about 0.36 eV and are independent on the surface passivants of AT molecules among the present OT-, DT-, and HDT-passivated Au nanoparticles. Moreover, these surface-potential shifts are found to be significantly smaller than that of AT SAMs on the Au substrates. This result is qualitatively explained by the difference of the shape of interface dipole layer.

This work was supported by a Grant-in-Aid from the Ministry of Education, Culture, Sports, Science and Technology of Japan. This work was also supported by grants from Hyogo Science and Technology Association and Kawanishi Memorial Shinmaywa Education Foundation. The synchrotron-radiation experiment was performed under the Joint Studies Program (2004 and 2005) of the Institute for Molecular Science. We thank T. Ito, S. Kimura, and the staff of the UVSOR II Facility, Institute for Molecular Science, for their technical support.

*Corresponding author. Electronic address: a-tanaka@mech.kobe-u.ac.jp

[1] M. P. A. Viegers and J. M. Trooster, Phys. Rev. B **15**, 72 (1977).
[2] G. Medeiros-Ribeiro, D. A. A. Ohlberg, R. S. Williams, and J. R. Heath, Phys. Rev. B **59**, 1633 (1999).
[3] M. Brust, M. Walker, D. Bethell, D. J. Schiffrin, and R. Whyman, J. Chem. Soc., Chem. Commun. **1994**, 801 (1994).
[4] M. M. Alvarez, J. T. Khoury, T. G. Schaaff, M. Shafigullin, I. Vezmar, and R. L. Whetten, Chem. Phys. Lett. **266**, 91 (1997).
[5] A. Taleb, V. Russier, A. Courty, and M. P. Pileni, Phys. Rev. B **59**, 13350 (1999).
[6] W. D. Luedtke and U. Landman, J. Phys. Chem. **100**, 13323 (1996).
[7] X. M. Lin, C. M. Sorensen, and K. J. Klabunde, J. Nanopart. Res. **2**, 157 (2000).
[8] A. Tanaka, Y. Takeda, M. Imamura, and S. Sato, Phys. Rev. B **68**, 195415 (2003).
[9] A. Tanaka, Y. Takeda, T. Nagasawa, and K. Takahashi, Solid State Commun. **126**, 191 (2003).
[10] T. C. Hsieh, A. P. Shapiro, and T.-C. Chiang, Phys. Rev. B **31**, 2541 (1985).
[11] P. H. Citrin, G. K. Wertheim, and Y. Baer, Phys. Rev. B **27**, 3160 (1983).
[12] M. Imamura and A. Tanaka, Phys. Rev. B **73**, 125409 (2006).
[13] M. Seidl, K.-H. Meiwes-Broer, and M. Brack, J. Chem. Phys. **95**, 1295 (1991).
[14] D. M. Alloway, M. Hofmann, D. L. Smith, N. E. Gruhn, A. L. Graham, R. Colorado, Jr., V. H. Wysocki, T. R. Lee, P. A. Lee, and N. R. Armstrong, J. Phys. Chem. B **103**, 11690 (2003).
[15] S. D. Evans and A. Ulman, Chem. Phys. Lett. **170**, 462 (1990).